



LAWRENCE
LIVERMORE
NATIONAL
LABORATORY

Reaching Isochoric States of Matter by Ultrashort-Pulse Proton Heating

P.K. Patel, A.J. Mackinnon, M. Allen, M.E. Foord, R. Shepherd, and D.F. Price

Feb 14th, 2005

LDRD Project 02-ERD-006 Final Report

Disclaimer

This document was prepared as an account of work sponsored by an agency of the United States Government. Neither the United States Government nor the University of California nor any of their employees, makes any warranty, express or implied, or assumes any legal liability or responsibility for the accuracy, completeness, or usefulness of any information, apparatus, product, or process disclosed, or represents that its use would not infringe privately owned rights. Reference herein to any specific commercial product, process, or service by trade name, trademark, manufacturer, or otherwise, does not necessarily constitute or imply its endorsement, recommendation, or favoring by the United States Government or the University of California. The views and opinions of authors expressed herein do not necessarily state or reflect those of the United States Government or the University of California, and shall not be used for advertising or product endorsement purposes.

Auspices Statement

This work was performed under the auspices of the U. S. Department of Energy (DOE) by the University of California, Lawrence Livermore National Laboratory (LLNL) under Contract No. W-7405-Eng-48. The project (02-ERD-006) was funded by the Laboratory Directed Research and Development Program at LLNL.

FY04 LDRD Final Report
**Reaching Isochoric States of Matter by Ultrashort-
Pulse Proton Heating**
LDRD Project Tracking Code: 02-ERD-006
Pravesh Patel, Principal Investigator

Abstract

The aim of this LDRD is to develop two completely new methods for creating and probing warm dense states of matter (plasmas at several eV at solid density), which will enable the direct measurement of fundamental material properties such as the opacity and equation of state (EOS). There is in this warm dense regime an almost complete lack of quantitative experimental data—primarily because of the difficulty in creating uniform, single temperature/density plasmas on which to make measurements. In an ideal case one would volumetrically heat a target with a very short burst of energy—simultaneously making measurements prior to the subsequent hydrodynamic expansion of the target. However, no mechanism for such rapid, uniform heating of a material currently exists. We propose to develop a completely new technique that has the potential for creating large uniform plasmas in local thermodynamic equilibrium (LTE) at warm dense conditions. This technique is based on volumetric heating of solid density targets with a high energy, high-flux, short-pulse, laser-produced proton beam. We also propose to use this beam of protons to probe high-Z, solid density matter with both 2-dimensional spatial resolution and picosecond temporal resolution. The combination of these two techniques will enable us to make the very first quantitative measurements of the equation of state and opacity of an isochorically heated state of matter.

Introduction/Background

A material heated at constant volume to high pressure follows—in EOS phase space—an isochor. When pressures and temperatures approach a few Mbar and a few eV respectively such materials enter a strongly-coupled partially-ionised regime commonly referred to as 'warm dense matter.' Existing as an intermediary state between cold materials and highly-ionised plasmas the warm dense matter regime is routinely encountered in most laboratory-produced plasmas as well as astrophysical bodies such as planetary cores. Such states lie in a region in density-temperature space which bridges those of solid room-temperature materials described by condensed matter theory, and high-temperature ionized plasmas described by classical plasma theory. The intermediate regime is not easily described by an extension from either of these well-established theoretical frameworks, and thus, has so far eluded a satisfactory theoretical description. Warm dense plasmas are characterized by strong ion-coupling, continuum lowering, partial degeneracy, and partial ionization. In such plasmas both short and long-range forces between ion-electrons and ion-ions are important, and the resulting many-body problem presents a formidable computational challenge. Current laboratory efforts are focused on the

development of first-principles theoretical EOS models and computationally-intensive molecular dynamics (MD) simulations.

Warm dense plasmas are also very challenging from an experimental perspective. Continuing experimental efforts to obtain high quality EOS data with which to benchmark or differentiate competing theoretical models are beset by the difficulties in both creating, and diagnosing, uniform, single-temperature, single-density plasmas in LTE. To date the approaches to access this regime have included gas-gun compression of bulk solids, direct laser-induced shock heating, and indirect x-ray heating inside a laser-driven hohlraum. However, gas-gun data are limited to fairly low pressures, and laser-based experiments struggle to contend with the sharp gradients produced through non-uniform heating—as well as requiring laser facilities on the scale of Nova, Omega, and NIF.

All of these methods produce spatial gradients. Ideally the study of warm dense matter can be done with a very short burst of energy that heats a target to some elevated temperature and pressure—with measurements performed prior to the subsequent expansion of the target. This has been attempted using direct short-pulse-laser heating of thin foils. The real difficulty with this approach is that to achieve uniform or volumetric heating the thickness of the foils must be comparable to the heating skin-depth of the laser, approximately 100 Å; however, these extremely thin foils expand on sub-picosecond timescales making measurements highly problematic. A substantial improvement in experimental capability dictates larger, thicker targets. This, in turn, necessitates a novel heating source.

In this LDRD we propose to investigate a new technique that has the potential for creating large uniform plasmas in LTE at warm dense conditions. This technique is based on long-range volumetric proton heating and arises from the discovery that a high intensity, short-pulse laser incident on a solid target can produce an intense, highly-directional, multi-MeV proton beam.

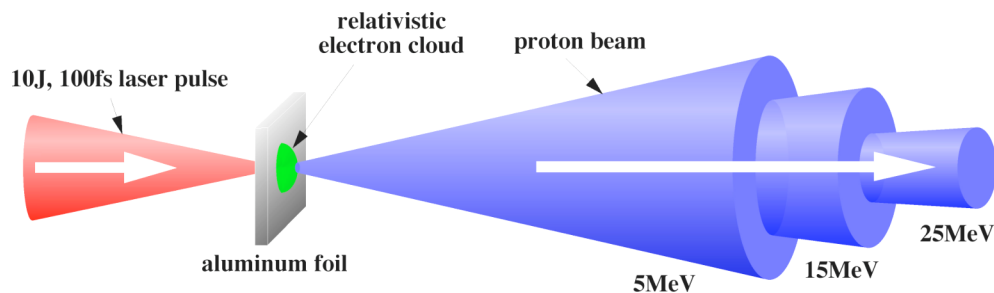


Fig. 1. Schematic of proton beam generation

A schematic of the process is shown in Fig. 1. An ultraintense laser pulse incident on a solid foil ponderamotively accelerates large numbers of electrons into the foil with relativistic energies. These electrons exiting the rear surface of the foil into vacuum set up an extremely high electrostatic field normal to the surface which drags out ions from the surface of the foil accelerating them to MeV energies. We performed an experiment on the 100 TW JanUSP laser¹ at LLNL in which we observed intense beams of protons with energies up to 25 MeV. The protons are emitted normal to the rear surface of the target, in a highly directional beam. With a laser intensity of

2×10^{20} W/cm² we have measured the absolute total energy in the protons above 5 MeV to be 66 mJ, giving a conversion efficiency of 0.7% of the incident laser energy.

Using the LASNEX rad-hydro code we investigated the feasibility of using this proton beam to heat a secondary target. Based on our experimentally measured proton flux at 5 MeV we calculate that a 50 μ m Cu cube placed 100 μ m from the target is heated almost instantaneously (< 3 ps) and uniformly ($< 20\%$) to a temperature of 8 eV. Over this heating time the entire sample remains at solid density (the edges of the Cu cube have expanded by < 0.1 μ m.)

We have further calculated the subsequent hydrodynamic motion of the sample. As the solid begins to expand a rarefaction wave propagates inwards from each boundary at the sound speed. The actual sound speed can be calculated from the EOS of the material. However, performing the calculation twice for two different but well-established EOS models for Cu give pressures at solid density of in one case 3.5 Mbar and in the other 5.0 Mbar. The resulting predicted sound speeds vary by approximately 50%. Thus, a measurement of the sound speed enables us to directly differentiate between competing EOS models.

To measure the sound speed, and to verify the uniformity of the target heating, one needs to probe the bulk solid material. Optical probing of a solid density metal is not possible. X-ray probing is a possibility but would require a very high flux of high energy x-rays to penetrate 50 μ m of material. Therefore, we propose a second use for the proton beam—to probe the bulk solid density plasma. The stopping or energy loss of protons through a material is sensitive to both density and ionization state. We will use the higher energy protons (20 MeV protons can penetrate through almost 1000 μ m of Cu) to probe the bulk plasma by point projection radiography.

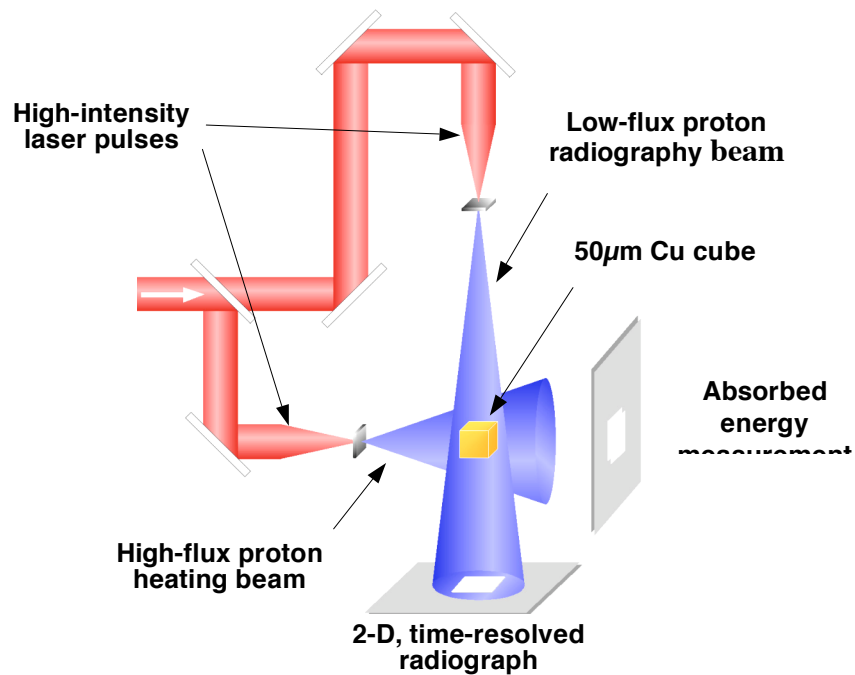


Fig. 2. Experiment to measure sound speed in a solid density, few eV plasma.

The experiment we propose to measure the sound speed in a uniform warm dense plasma, and thus obtain the equation of state, is shown schematically in Fig. 2. We plan to use two short-pulse, high-intensity laser beams to create two proton beams—one to isochorically heat the sample and a second to probe it. This experiment, if successful, would provide the first experimental data on the equation of state of any material on its isochor.

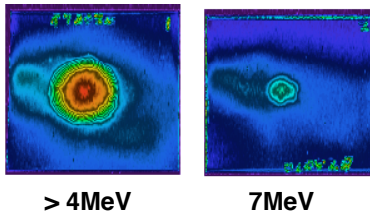
The goals we set out in this proposal are extremely challenging both from a scientific and technical standpoint. They rely on the successful development of two completely untried experimental techniques; one to use an intense burst of protons to uniformly and isochorically heat a solid density, high-Z material, and a second to proton radiograph the material with high spatial and temporal resolution.

Results/Technical Outcome

The first set of experiments were performed in Nov/Dec 2001 on the 100TW JanUSP laser at LLNL with the purpose of:

- (a) optimizing the flux of the laser-produced proton beam,
- (b) resolving the remaining issues concerning the proton production and acceleration mechanisms, and
- (c) testing the viability of probing solid density materials with high energy protons.

(a) 100 μ m



(b) 3 μ m

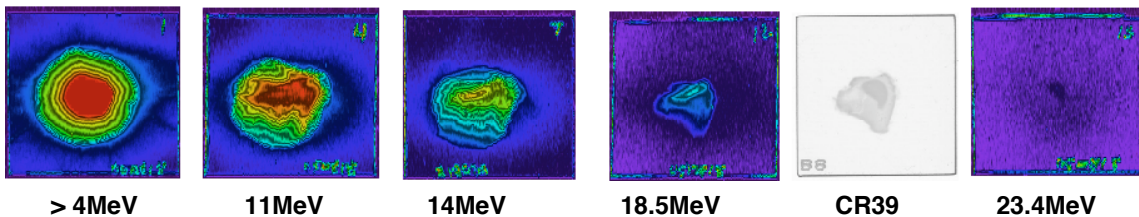


Fig. 3. Proton beam recorded on Radiochromic Film (RCF) from targets of 3 μ m and 100 μ m thickness

Figure 3 shows the proton beam recorded with RCF for shots of varying target thickness. The beam shows a strong dependence on both target material and target thickness. The flux was found to increase dramatically with decreasing target thickness, particularly below 15 μ m, with the maximum flux observed from 3 μ m foils. Subsequent particle-in-cell (PIC) simulations (shown in Fig. 4) showed that this strong dependence arises from the effect of hot electron re-circulation within the foil

which enhances both the electron density and accelerating electrostatic field on the rear surface of the target.

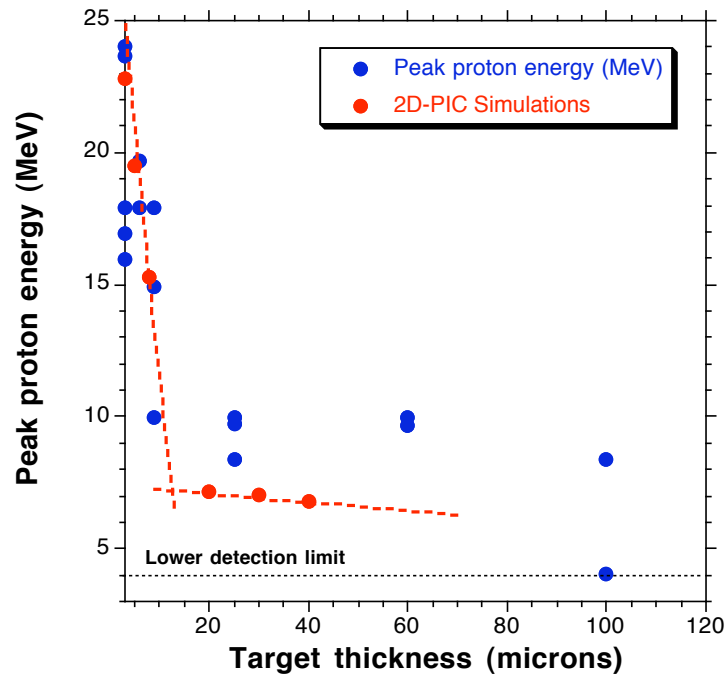


Fig. 4. Peak proton energies as a function target thickness. Blue dots represent data points; red points results of a 2D PIC calculation.

This is the first time such an effect has been observed either experimentally or in simulation—this work was published in Physical Review Letters in 2002.²

The initial experiments to test the technique of proton probing on solid sample objects also produced encouraging results. We radiographed a variety of test objects using two primary detectors; radiochromic film (RCF), and CR-39 nuclear track detectors. Figure 5a. shows a radiograph in RCF of a 22 μ m thick aluminum foil with a 1 μ m peak-to-valley sinusoidal imprint on one surface. This RCF detector layer corresponds primarily to protons of 6MeV in energy.

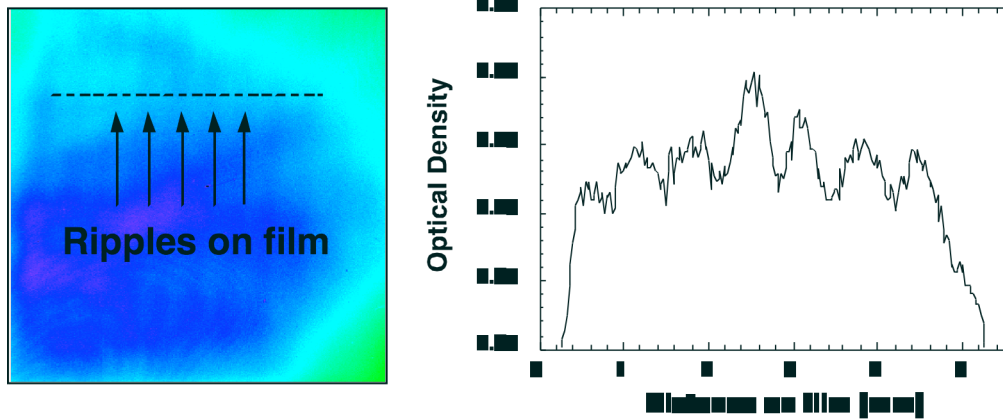


Fig. 5. (a) Proton radiograph of a 22µm thick aluminum foil imprinted on one side with a 1µm peak-to-valley 1-D sinusoidal pattern, and (b) horizontal lineout across film.

The lineout in Fig. 5b. clearly shows the sinusoidal imprint on the foil. The contrast in optical density on the film matches approximately to the 4% variation in the foil thickness produced by the sinusoidal imprint. These preliminary results indicated that the proton probing technique would enable us to resolve density variations below the few percent level in thick mid-Z and high-Z samples.³

In FY03 we progressed from our previous FY02 proton characterisation and optimisation studies to the first set of actual proton heating and proton radiography experiments. In a campaign on the 100fs JanUSP laser at LLNL we demonstrated (i) the first successful focusing of a laser-generated proton beam—increasing its flux density by almost an order of magnitude, and (ii) the first successful isochoric heating of a material with an ultrafast proton beam. The experimental setup is shown in Fig. 6a.

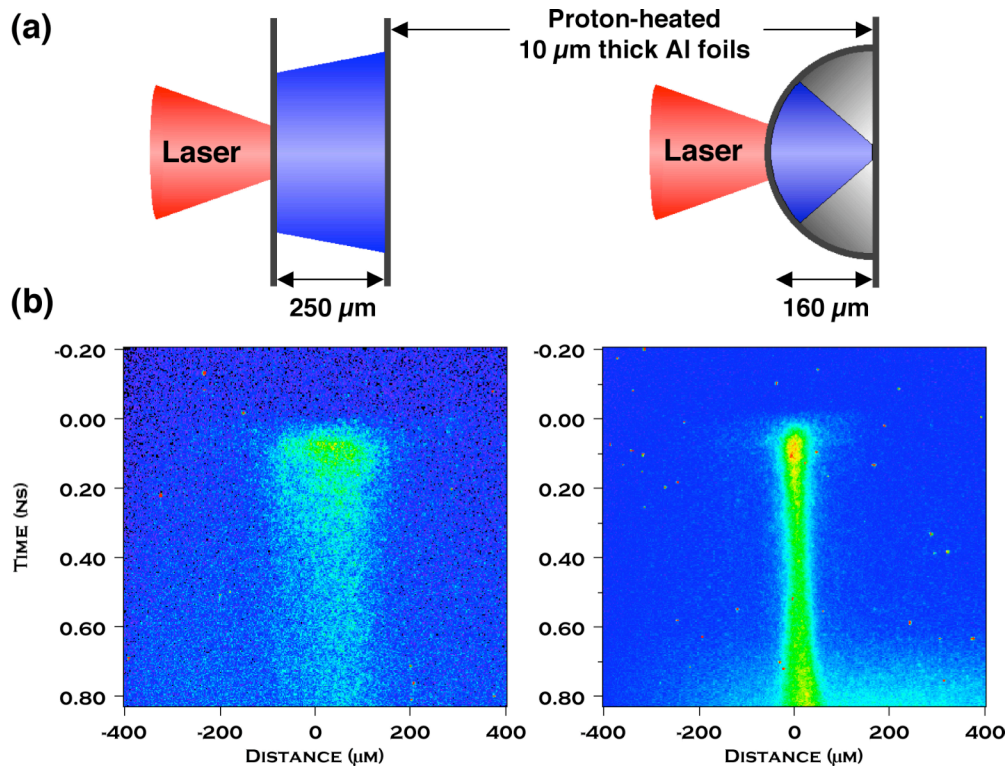


Fig. 6 (a) Schematic of target geometries for unfocused and focused proton beam, and (b) corresponding streaked images of thermal emission from rear of heated targets.

A planar case was studied first in which the proton beam is produced from a 10 μm planar Al foil, and a second 10 μm Al foil is placed behind the first at a distance of 250 μm. In the focusing case the proton beam is produced from a 10 μm thick, 320 μm diameter hemispherical Al shell, and a second 10 μm Al foil is placed in a plane coinciding with the geometric center of the shell. The temperature of the proton heated foil was determined with a fast optical streak camera recording Planckian thermal emission from the hot rear surface. An absolute single wavelength measurement was made using a 570 nm interference filter. The overall temporal and spatial resolution was 70 ps, and 5 μm, respectively. The 10 μm thick proton heated foil blocked any direct light from the primary laser-irradiated target.

The streak camera data obtained for the two target geometries, each with 10 J of laser energy incident on target, are shown in Fig. 6b. For the planar foil case (left image) we observe quite uniform emission from a large area of the secondary foil (186 μm FWHM). The onset of the emission is rapid—shorter than the time resolution of the streak camera—and decreases slowly over the following 800 ps. This temporal behavior (a rapid rise with a slow fall-off) is consistent with that from a body which is heated isochorically to some temperature and which then under its own pressure expands and cools. The spatial extent of 186 μm is in good agreement with our measurement of the maximum proton source size of approximately 250 μm at the lowest recorded proton energy (NB. the protons primarily responsible for the heating at a depth of 10 μm have energies in a band around 0.9 MeV). With the hemispherical foil (right image) we observe a dramatic reduction in the size of the

heated region (46 μm FWHM) coupled with a marked increase in the emission intensity (approximately a factor of 8). The factor of 4 reduction in the spatial extent in one dimension corresponds to a 16 times smaller heated area.

An interferometer was used to simultaneously monitor the foils for signs of plasma formation. The interferometry beam was a frequency-doubled 100 fs pulse directed along the target surface and timed to arrive 180 ps after the main pulse. Figure 7 shows the interferogram for the 320 μm hemispherical shell target corresponding to the same shot shown in Fig. 6b. The large fringe shifts on the left of the target arise from the blow-off plasma covering the outer surface of the hemispherical shell (the laser is incident from the left). The right side of the image corresponds to the rear surface of the secondary foil. A small region of expanding plasma is clearly visible. The plasma, originating from the rear surface, is centered along the central axis of the hemisphere, and extends laterally over approximately 50 μm , in good agreement with the 46 μm heated region measured with the streak camera. Taken together these observations provide a strong indication of the ballistic focusing of the proton beam, and of the corresponding enhancement in its flux density.

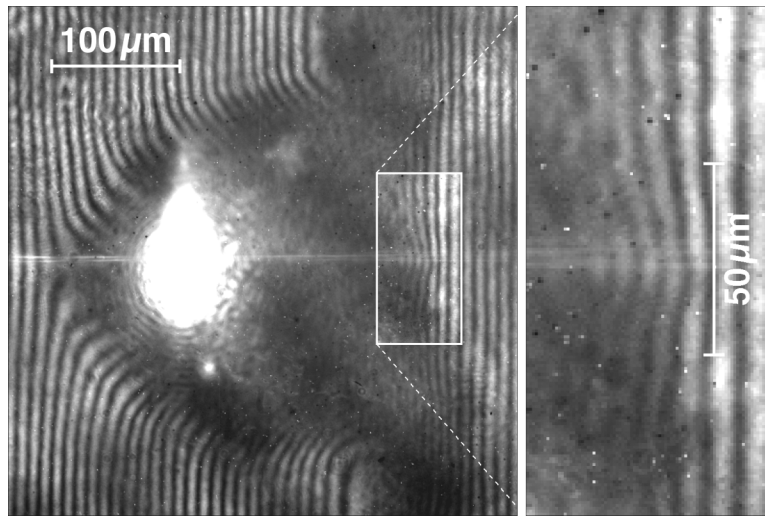


Fig. 7. Interferogram of focusing target shot taken 180 ps after incidence of the main pulse. The enlarged image on the right shows an approximately 50 μm region of expanding plasma originating from the rear surface of the proton heated foil.

An absolute single wavelength intensity measurement of the rear surface emission enables us to estimate the rear side temperature of the proton heated foil. Absolute calibration of the streak camera and transmission optics in the beam path provided an overall accuracy of $\pm 25\%$. The radiation-hydrocode LASNEX was used to model the hydrodynamic expansion and optical emission of the foil, assuming it to be instantaneously heated to some initial temperature. The simulated emission at 570 nm from the rear surface was then compared with the absolute intensity measurements.

Taking lineouts from the two images in Fig. 6b we obtain peak emission values of 5.7×10^{14} and 4.3×10^{15} $\text{ergs s}^{-1} \text{cm}^{-2} \text{keV}^{-1}$ respectively. Fitting to these peak values

LASNEX modeling indicates for the planar heating case an initial temperature of the Al foil of 4 ± 1 eV, and for the focused heating case a temperature of 23 ± 6 eV. The comparison between experiment and simulation for this latter case is shown in Fig. 8. We note that the fall-off in the emission intensity over the first 400 ps matches the data very closely. Since both the peak intensity and the fall-off are strong functions of the plasma temperature, this good agreement gives us an added degree of confidence in the accuracy of the temperature measurement. The rise in signal at 400 ps may be due to gradient effects from the front of the foil such as a shockwave reaching the rear surface.

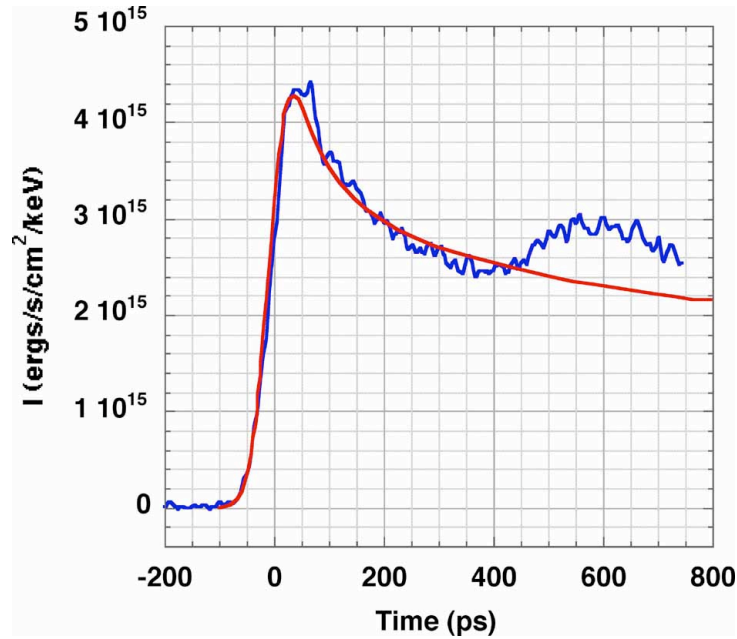


Fig. 8. Comparison of time-dependent experimental (blue) and simulated (red) emission intensities for hemispherical target shot. The experimental curve is a temporal lineout spatially-integrated over the $46\ \mu\text{m}$ FWHM of the signal. The simulated curve is a LASNEX calculation of the $570\ \text{nm}$ emission from a $23\ \text{eV}$ solid density Al plasma.

The proton beam flux required to heat the foils to the observed temperatures was estimated using a Monte Carlo simulation⁴. Protons with an exponential energy spectrum of $1.5\ \text{MeV kT}$ were injected into a $10\ \mu\text{m}$ thick Al foil. Energy loss and energy deposition as a function of distance were computed. The energy deposition at a depth of $10\ \mu\text{m}$ was found to be $9.2\times 10^{-7}\ \text{J/g}$ per incident proton. Comparing to the evaluated energy density of $7.3\times 10^5\ \text{J/g}$ at $23\ \text{eV}$ requires a total of 7.9×10^{11} protons focused to the observed $46\ \mu\text{m}$ diameter spot. The total energy in such a distribution is $190\ \text{mJ}$, or 1.8% of the incident laser energy. Although approximate, this figure is entirely consistent with our previous estimates of a $1\text{-}2\%$ conversion efficiency to protons, showing that there is sufficient energy in the focused proton beam to induce isochoric heating to the level observed.

The focusing in a purely ballistic limit can be estimated by considering the flow angle deviation with source radius, as seen from a planar foil, and applying it to the

hemispherical shell. The real behavior is expected to deviate from a pure ballistic case because of the spatio-temporal varying electron density and accelerating sheath field at the target rear surface. To gain insight into the complex focusing dynamics we carried out 2-D particle-in-cell (PIC) simulations which model the laser absorption, electron generation and propagation, and proton acceleration. A spatio-temporal Gaussian pulse with 50 μm and 100 fs FWHM, respectively, is incident at the left boundary of a 200 \times 200 μm simulation box. The resulting peak laser intensity is $5 \times 10^{18} \text{ Wcm}^{-2}$. The target consists of a 10 μm thick, 125 μm radius Al shell with a 10 μm thick flat Al foil positioned at the centre of curvature of the shell. A 0.1 μm H layer is added to the inner surface of the hemisphere to simulate the proton-producing hydrocarbon layer.

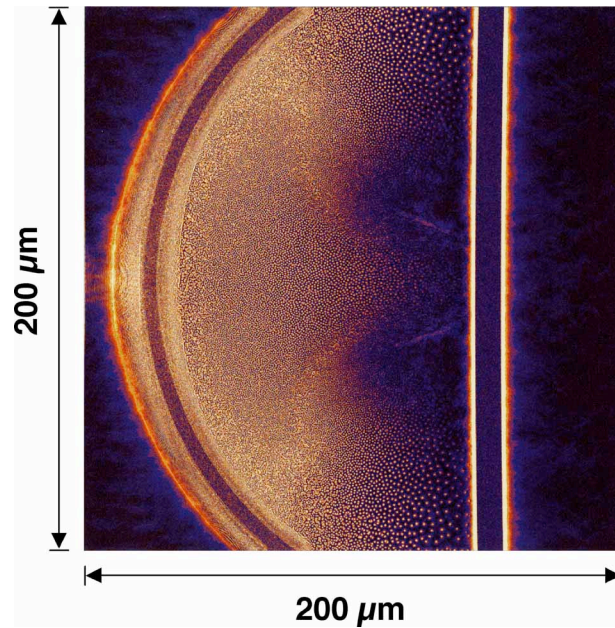


Fig. 9. Particle-in-cell (PIC) calculation of the electric field density at 3.4 ps for a $5 \times 10^{18} \text{ Wcm}^{-2}$ intensity laser pulse incident on a 250 μm diameter, 10 μm thick hemispherical Al shell.

Figure 9 shows a result from the simulation, an electric field density map at a time 3.4 ps after the peak of the laser pulse. At this time the leading edge of the ion front has almost reached the rear foil. The accelerating sheath field can be seen to cover a large area of the inner surface of the hemisphere, producing a substantial degree of directed proton acceleration. This work was published in Physical Review Letters in 2003.⁵

Our first multi-beam experiment in which we were able to directly probe a laser-produced plasma with a proton beam was performed at the LULI facility at Ecole Polytechnique, France. We used a single 70J long-pulse beam to generate a shock in a 15 μm thick Al foil. For some shots an EOS sample of Quartz or CH was glued to the rear of the Al foil. A VISAR was used to monitor the shock breakout through the EOS sample. A 25J, 350fs pulse generated a proton beam which was used to radiograph the foil side-on. The proton radiograph, in point-projection, provides a few micron

spatial resolution combined with picosecond time resolution. Figure 10a. shows a proton radiograph of a shocked Quartz sample. Although a variation in the proton flux density can be seen through the material we found that the contrast and spatial resolution (approximately 60 microns) was too low to observe a density jump within the sample. The relatively poor spatial resolution arises from multiple scattering within the sample. It can be significantly improved by reduced sample size, and higher proton energies.

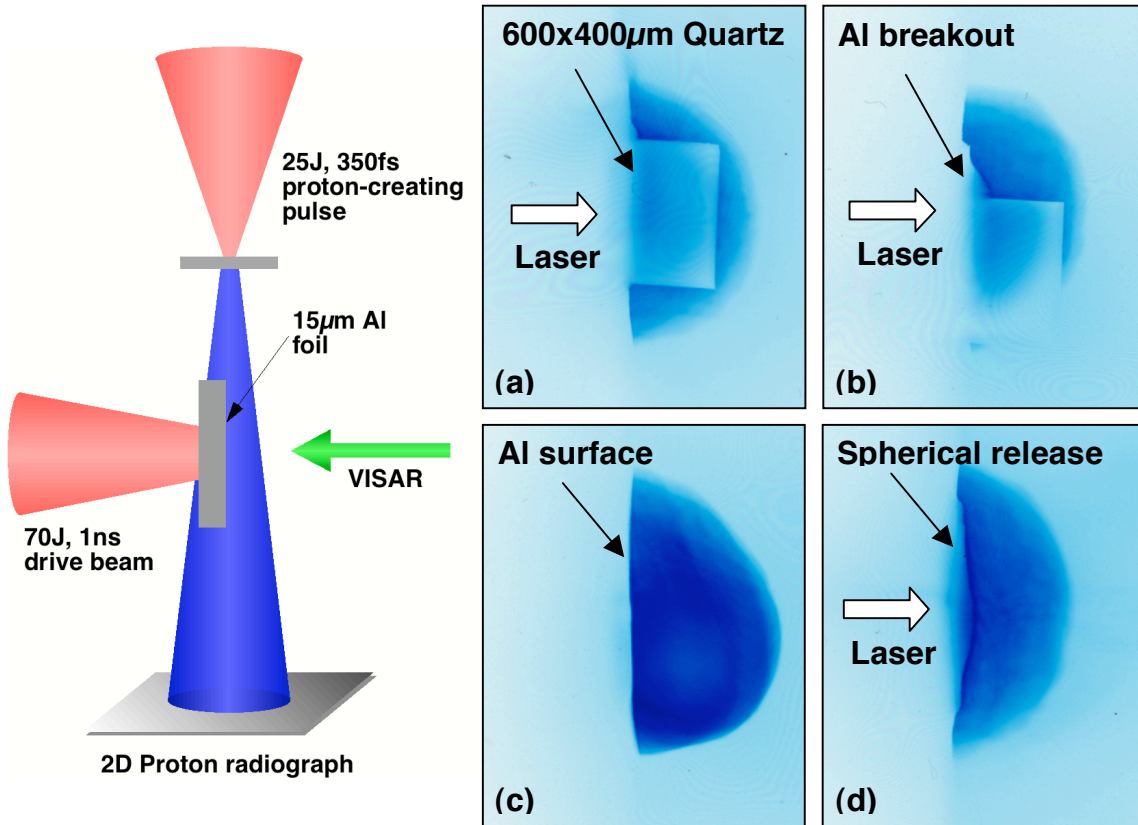


Fig. 10. Experimental setup and data from proton radiography of an Equation of State shock experiment. (a,b) Proton radiographs through a shocked Quartz sample. (c) Proton radiograph of an unshocked 15µm Al foil. (d) Proton radiograph of a shocked 15µm Al foil, showing shock breakout at rear surface.

As an alternative to probing inside the sample we attempted to probe the shock release at the rear of the Al foil. Figures 10c. and d. show proton radiographs of an unshocked and shocked Al foil respectively. A clear deflection is seen in the proton beam at the rear surface of the foil. The deflection shows a fairly spherical release at the rear surface consistent with simultaneous VISAR interferometric measurements of the rear surface shock breakout. We are performing Monte-Carlo proton scattering modeling to reconstruct the density profile of the release.⁶

Although in this project we successfully created isochorically heated plasmas in the 10-20eV range we found that the spatial resolution of the proton probe beam able to be created on the JanUSP laser would be insufficient to probe a density front in solid

material to the degree required for an accurate EOS measurement. Recent experiments performed with collaborators at LLNL⁷ on high energy K-alpha x-ray production have suggested that it may be possible to generate an x-ray source with sufficiently high energy, and sufficiently small source size, to radiograph the density front in an isochorically heated material. This method is currently being studied as an alternate means of achieving our goal of measuring the EOS in an isochorically heated material.

References

- ¹ J.D. Bonlie, F. Patterson, D. Price, B. White, and P. Springer, *Appl. Phys. B Suppl.* **70**, S155 (2000)
- ² A.J. Mackinnon, Y. Sentoku, P.K. Patel, D. Price, S. Hatchett, M.H. Key, C. Andersen, R. Snavelly, and R.R. Freeman, *Phys. Rev. Lett.* **88**, 215006 (2002)
- ³ M. Borghesi, A.J. Mackinnon, D.H. Campbell, D.G. Hicks, S. Kar, P.K. Patel, D. Price, L. Romagnani, A. Schiavi, and O. Willi, *Phys. Rev. Lett.* **92**, 055003 (2004)
- ⁴ J.F. Ziegler, J.P. Biersack, and U. Littmark, *The Stopping and Range of Ions in Solids*, Pergamon Press, New York (1996)
- ⁵ P.K. Patel, A.J. Mackinnon, M.H. Key, T.E. Cowan, M.E. Foord, M. Allen, D.F. Price, H. Ruhl, P.T. Springer, and R. Stephens, *Phys. Rev. Lett.* **91**, 125004 (2003)
- ⁶ M. Koenig, E. Henry, G. Huser, A. Benuzzi-Mounaix, B. Faral, E. Martinolli, S. Lepape, T. Vinci, D. Batani, M. Tomasini, B. Telaro, P. Loubeyre, T. Hall, P. Celliers, G. Collins, L. DaSilva, R. Cauble, D. Hicks, D. Bradley, A. Mackinnon, P. Patel, J. Eggert, J. Pasley, O. Willi, D. Neely, M. Notley, C. Danson, M. Borghesi, L. Romagnani, T. Boehly, and K. Lee, *Nucl. Fusion* **44**, S208-214 (2004)
- ⁷ H-S. Park, N. Izumi, M.H. Key, J.A. Koch, O.L. Landen, P.K. Patel, and T. W. Phillips, *Rev. Sci. Instr.* **75**, 4048 (2004)